

---

# 3D CFD Simulation of the Thermal Performance of an Air Channel Solar Heater

Samir Moujaes and Jayant Patil

---

## 1 Introduction

Over last few years there has been a growing interest in the field of solar air heaters for solar assisted crop drying technique. Drying is a process of heat transfer to the product from a heating source. Solar energy allows various ways to construct a system and thereby it possesses a mode which can necessitate a simple technology for a particular usage and for a particular region. In this study at hand Las Vegas, Nevada is considered as potential region of interest for use of this type of heaters but for residential applications. Solar air heaters are the devices employed to gain useful heat energy from incident solar radiation. Solar collectors can be of concentrating or flat plate type. For solar energy crop drying applications or residential applications flat plate collectors provide the desired temperature ranges.

Several designs of the solar air heaters had been proposed in the past. Among the recent ones [1] presented the concept of applying different heat sources for agricultural drying applications using six different natural circulation solar air collectors. Each of the collectors has combinations of glazing and different types of absorber plates such as zigzag, flat plate, front pass, back-pass etc. [2] performed the analysis of multi-tray crop drying attached to an inclined multi-pass solar air heater with in-built thermal storage. Another work [3] provided an optimization method for agricultural drying using forced convection hot air dryer. Another paper [4] reported on the design of a solar dehydrator for agricultural crops in India. The unit consists of solar air heater and a drying chamber. The study focuses on calculating the drying ratio and rehydration ratio. Finally [5] analyzed a solar air collector with different heat transfer coefficients in the collector and within the external environment. The study is

aimed to calculate the fluid outlet temperature, efficiency as the function of wind speed, incident solar radiation and mass flow rate.

A review of these previous research works did not reveal any work using CFD simulations for the purpose of predicting the performance of any of these solar air heater designs which is the reason for this study and to show the flexibility and the power of using a computational fluid dynamics for the purpose of initial evaluation of scoping designs.

---

## 2 Physical Model

Fig. 1 shows the physical model simulated. The dimensions of the collector are 0.85 m x 1.22 m (W x L). The height of the solar collector is 16.5 cm. The top cover of the collector is made of transparent glass (0.3175 cm thick). The insulation material for the collector is glass wool. The sides and the bottom of the collector are insulated with 5.0 cm thick layer of glass wool. The surfaces of this cavity heat up and eventually impart heat to the flowing air through that volume. This is a first attempt at the CFD simulation to double check and make sure that the model is giving reasonable data for exist temperatures of the air as it exists from the other end of the cavity. The inside of the cavity walls are assumed to be painted with a dark color paint to enhance the radiation exchange between the surfaces and the air.

---

## 3 Theoretical Model

In this study we have simulated a three dimensional, single pass solar air heater model using a computational fluid dynamic approach STAR-CD. The analysis is performed for a summer day (June 21) for Las Vegas region in Nevada.

The ASHRAE Clear Sky Model [9] is used to calculate the value of solar irradiation at the earth's surface for five different times of day for this simulation (6 AM, 9 AM, 12 noon, 3 PM, 6 PM).

---

S. Moujaes (✉) • J. Patil  
ME Department, University of Nevada Las Vegas,  
Las Vegas, NV 89154-4027, USA  
e-mail: [samir.moujaes@unlv.edu](mailto:samir.moujaes@unlv.edu)

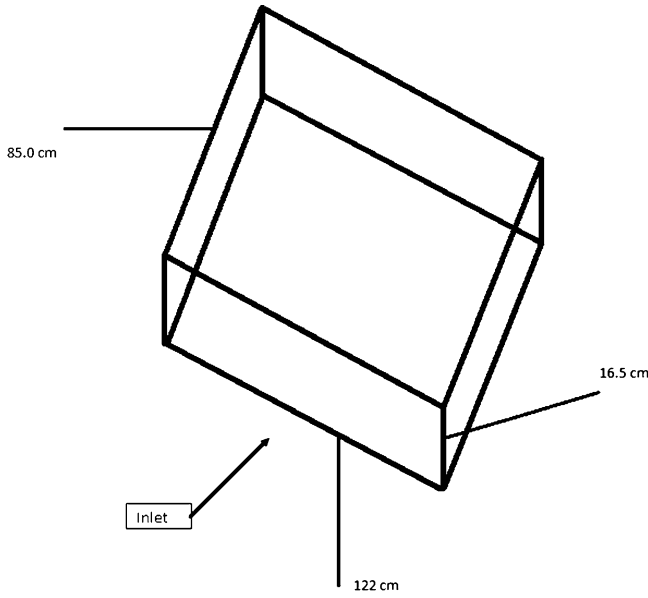


**Fig. 1** Schematic Diagram of Solar air collector

The equations to calculate the total solar radiation on vertical and horizontal surfaces are given below[9]:

(a) Total solar radiation incident on a **vertical surface**

$$G_t = G_D + G_d + G_R \quad (1)$$

The direct radiation corrected for clearness is given by

$$G_D = G_{N*D} * \max(\cos \theta) \quad (2)$$

For vertical surfaces the diffuse sky radiation is given by

$$G_d = \frac{G_{dV}}{G_{dH}} * C * G_{ND} \quad (3)$$

The rate at which energy is reflected onto the wall is given by

$$G_R = G_{tH} * \rho_g * F_{wg} \quad (4)$$

The value of the solar irradiation at the surface of the earth on a clear day is given by

$$G_{ND} = \frac{A}{\exp\left(\frac{B}{\sin \beta}\right)} * C_N \quad (5)$$

The ratio of diffuse sky radiation on a vertical surface to that incident on a horizontal surface on a clear day is given by

$$\frac{G_{dV}}{G_{dH}} = 0.55 + 0.437 * \cos \theta + 0.313 * \cos^2 \theta \quad (6)$$

The configuration or angle factor from wall to ground is

$$F_{wg} = \frac{1 - \cos \alpha}{2} \quad (7)$$

The rate at which the total radiation strikes the horizontal surface or ground in front of wall is given by

$$G_{tH} = (\sin \beta + C) * G_{ND} \quad (8)$$

(b) Total solar radiation on a **horizontal surface** is

$$G_t = \left[ \max(\cos \theta) + C * F_{ws} + \rho_g * F_{wg} * (\sin \beta + C) \right] * G_{ND} \quad (9)$$

The fraction of energy that leaves the surface and strikes the sky directly is given by

$$F_{ws} = \frac{1 + \cos \alpha}{2} \quad (10)$$

## 4 Computational Model

The computational analysis is performed using a steady state solution method for each of the five times of the day mentioned above as it is assumed that the thermal capacitance for this system is rather small and hence steady state conditions are achieved rather quickly at each hour of solar insolation exposure.

The physical problem comprises of heat transfer between the collector side and outside air is considered on the top and bottom of the collector, conjugate heat transfer property of the simulation software is employed during the analysis. Glass wool is used as the material of insulation on the outside of the solar collector. The CFD model takes into account the calculation concerned with the glass cover. The STAR-CD package has in built glass property section which gives the scattering and absorption coefficient of glass. The solar radiation which falls on top of the glass cover is the total heat gain for the solar air collector to heat the moving air inside it. A turbulent k-ε model is used for the analysis because of the Reynolds number (~14,000) is considered turbulent for a rectangular channel. The channel is assumed to be oriented with its air flow moving in a N-S orientation. Some parts of the solar collector are subjected to shading due to the vertical walls and are considered as such at the appropriate times of the day. To account for this shading caused by the walls, separate calculations for the shading calculations are included in the model (for each run) which depicts the portion of the area that is under shade and the one which is in direct sunlight for any particular time of the day. The velocity of air at the inlet of the solar collector

is assumed to be 0.74 m/s. The model is analyzed with a solution tolerance limit of  $10e-4$ . The numbers of nodes used in the model are 250,000 to insure grid independency. The cells of the computational model are chosen to be cubical in shape.

When the solution is converged the computational model generates an information file which predicts the enthalpy difference between the inlet and outlet of the collector. The final temperature (mean bulk temperature as calculated at the exit cross-section by STAR-CD) of the air moving exiting the collector is calculated as [8]:

$$\Delta H = \dot{m} * C_p * \Delta T \quad (11)$$

$$\Delta H = \dot{m} * C_p * (T_{in} - T_{out}) \quad (12)$$

The efficiency of the collector is calculated as

$$\eta_{th} = \frac{\Delta H}{W} \quad (13)$$

Where  $\Delta H$  is the change in energy from inlet to outlet and  $W$  is the amount of heat flux calculated from the ASHRAE clear sky model incident for that particular time of the day on the glass cover.

The value of the heat transfer coefficient on the exterior of the collector is calculated as [8]:

$$h = \frac{x_1}{k_1} + \frac{x_2}{k_2} \quad (14)$$

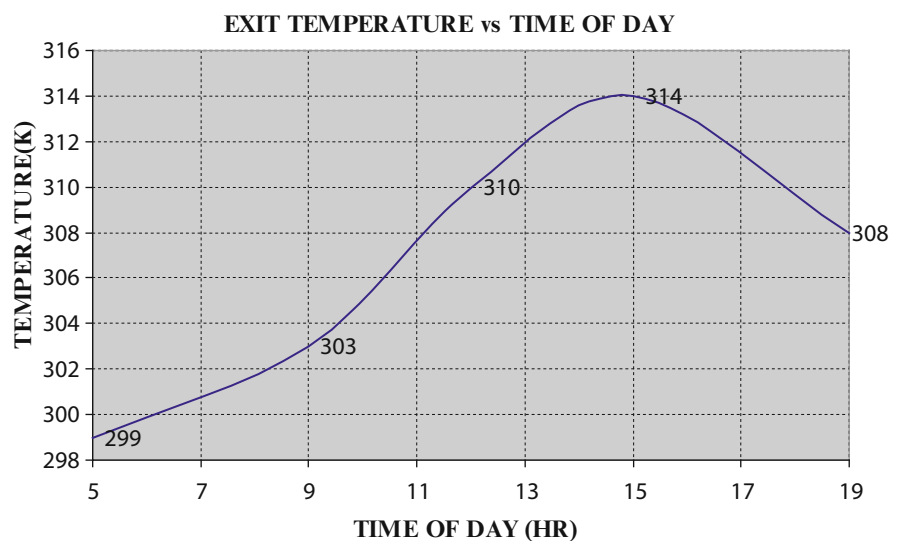
Where  $x$  and  $k$  are the thickness and the thermal conductivity of solar collector material and insulation material respectively.

## 5 Results and Discussion

Fig. 2 shows the results of the bulk averaged temperature across the exit cross section of the air heater for the five times of the typical simulation day used in this study. The plot indicates a gentle rise in that temperature initially till about 9 AM and then a much steeper rise till about 3:00 PM where that temperature is maximum and then a rapid decline of its value as the late afternoon hours progress. Although the insolation values are usually expected to maximize at around noon the ambient temperature is still increasing till late in the afternoon which is why it partially explains the time shift in that maximum value from solar noon.

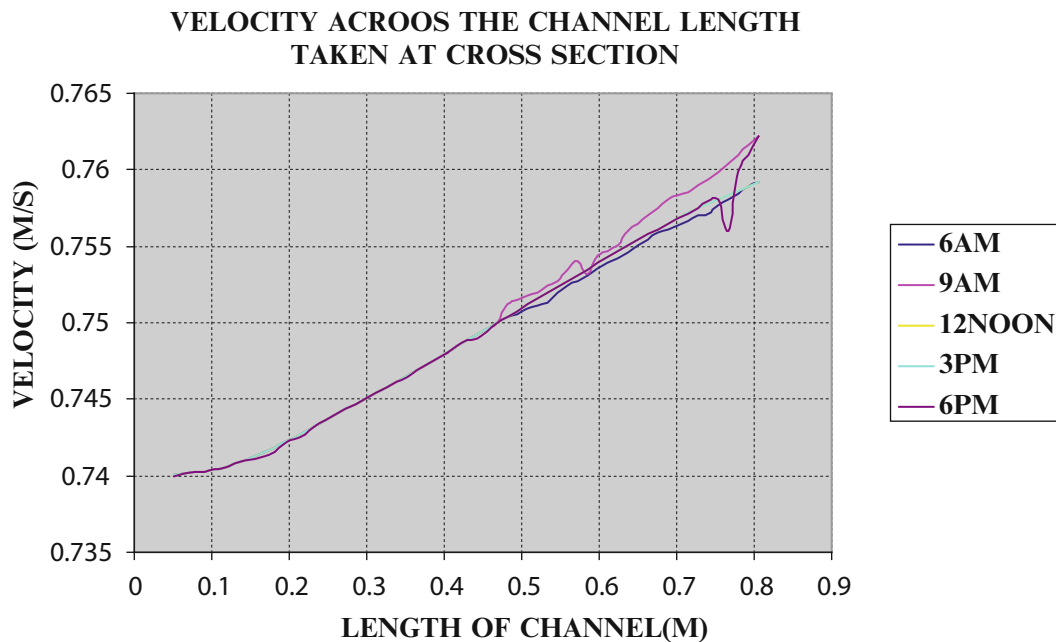
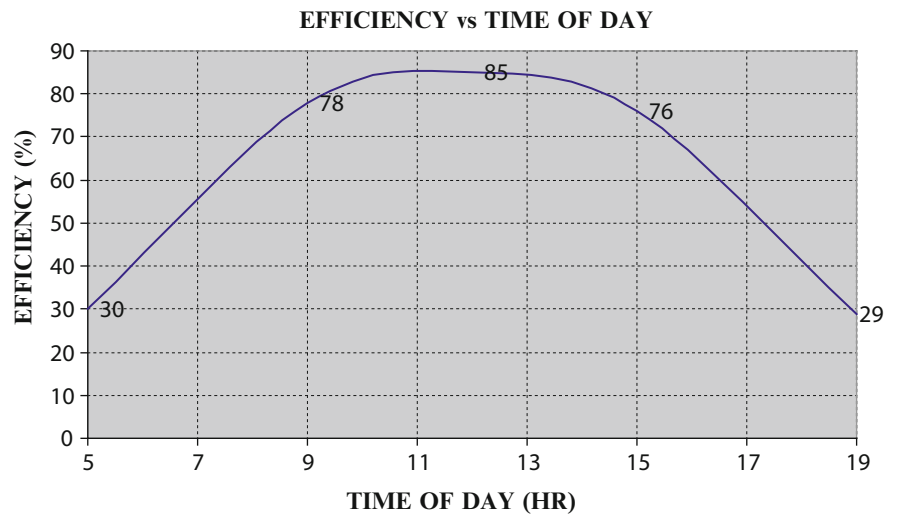
Fig. 3 shows the variation of the thermal efficiency as defined in equation (13). It shows that the value of  $\eta_{th}$  it shows that the efficiency is small at the start of the day indicating that the magnitude of the losses is large with respect to the total insolation on the air heater. AS the day progresses these losses although the grow larger but don't exceed the gains of heat into the air heater medium. That efficiency is maximized and stays flat over a period of roughly 9:00 AM till 3:00 PM in the afternoon indicating a stabilization between the heat losses and inputs to the system. Towards the latter part of the afternoon a steady decrease is seen from a valued of about 76 % till around 30 % due to the fact that in the late afternoon the sun's rays are at a higher inclined angle than at noon hence more reflection and ambient temperature also start decreasing as well increase the total heat losses relatively speaking.

Fig. 4 shows a localized plot of the axial velocity along the central axis of the channel's flow. It shows a slight increase of that velocity due to the effects of boundary



**Fig. 2** Exit air temperature at five different times of the day (6 AM, 9 AM, 12 noon, 3 PM, 6 PM)

**Fig. 3** Efficiency of the solar air collector for the five different times of the day



**Fig. 4** Velocity profile taken at cross section of channel from inlet to exit

layer flow on the wall boundaries as well as some instability toward the exit locations probably due to the exit conditions affecting some of the upstream flow. Again for most of the plots during the different times of the day the velocity along this axis does not show major variations as the air is assumed to be an incompressible fluid at these temperatures and pressure conditions. As mentioned earlier in the paper the assumed inlet velocity was taken to be a uniform value across the inlet at 0.74 m/s.

Finally Fig. 5 shows a plot of the pressure variation at the same axial location mentioned in Fig. 4. As one would expect there are no significant pressure drops in the air

flow at these average velocities as air has a relatively low density and viscosity that would not incur any major pressure drops. This is shown in Fig. 5 as a horizontal line for all the runs indicating a small variation as expected.

## 6 Conclusion and Future Work

The results of the CFD study shown above shows the potential of using this approach to adequately describe the trends and performance of a solar air heater adequately. Various design features can be added to the basic design to

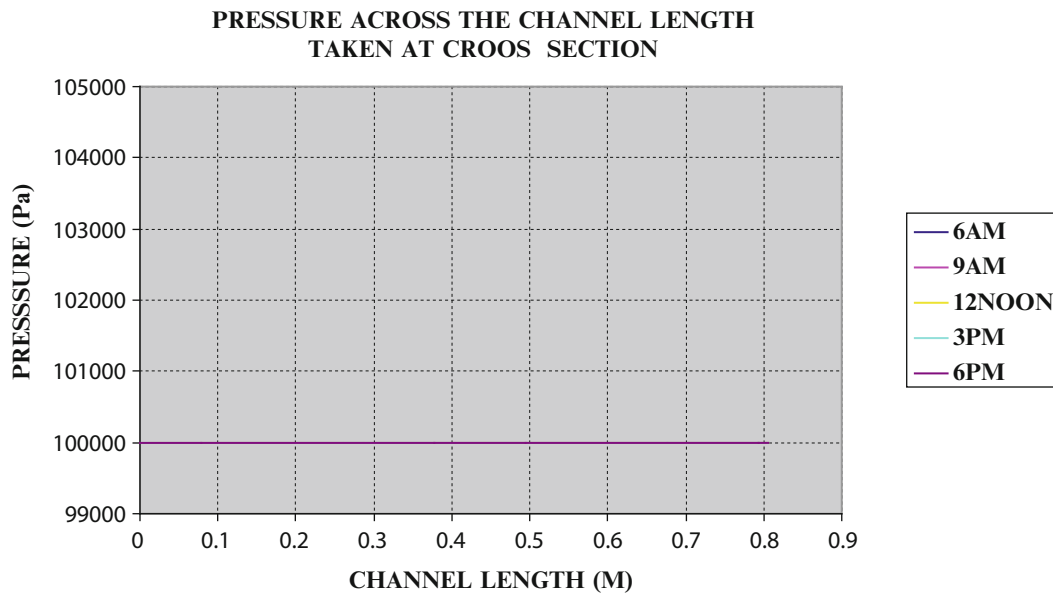


**Fig. 5** Pressure profile taken at cross section of channel from inlet to exit

accommodate the different unique features the various designer might envision to increase its thermal efficiency. The CFD results of this study match closely with the experimental work done by Othman, Yatim, et. On a double pass solar air collector.

The double pass solar air collector has curve shaped solar plates which are black in color where as in the current CFD study only plane baffles are used. The solar collector plates in double pass solar collector are located on either side of the medium separating the flows which in turn increases the efficiency. Still with the single pass, CFD study shows that the results are in close agreement with the double pass solar air collector.

Future work would include a more automated method of calculating the solar insolation at various times of the day for different locations and would incorporate the varying reflected sunlight at those times of day so that the net transmitted solar heat is calculated at each different time. In a future development a study of how naturally convected air through the solar air heater can be also incorporated which can be used to study a variety of flow situations.

## Nomenclature

$G_t$	Total solar radiation incident on surface ( $w/m^2$ )
$G_D$	Direct radiation corrected for clearness ( $w/m^2$ )
$G_d$	Diffuse sky radiation ( $w/m^2$ )
$G_R$	Rate of reflected energy ( $w/m^2$ )
$G_{ND}$	Normal direct irradiation ( $w/m^2$ )
$\theta$	Angle of incidence

$G_{dV}/G_{dH}$	Ratio of diffuse sky radiation for a vertical wall to horizontal surface
$C$	Clearness number
$G_{tH}$	Rate at which total radiation strikes surface in front of wall ( $w/m^2$ )
$\rho_g$	Reflectance
$F_{wg}$	view factor
$A$	Apparent solar irradiation ( $w/m^2$ )
$B$	Atmospheric extinction coefficient
$\beta$	Solar altitude
$\alpha$	Tilt angle
$F_{ws}$	Fraction of energy that leaves surface and strikes sky directly ( $w/m^2$ )
$\Delta H$	Enthalpy difference
$m$	Mass flow rate( $kg/s$ )
$h$	Heat transfer coefficient( $w/m^2.k$ )
$x$	Thickness of insulation(m)
$k$	Thermal conductivity( $w/m^2.k$ )
$\eta_{th}$	Thermal efficiency as defined in eq. (13)
1,2	solar heater material index and insulation material index

## References

1. Koyunchu, T: Performance of various designs of solar air heaters for crop drying, applications *Renewable Energy*, v 31, n 7, p 1055-1071, June 2006
2. Dilip, J: Modeling the system performance of multi-tray crop drying using an inclined multi-pass solar air heater with in-built thermal storage, *Journal of Food Engineering*, v 71, n 1, p 44-54, November 2005

3. McDoom, I.A.; Ramsaroop, R.; Saunders, R.; Tang Kai, A.: Optimization of solar crop drying, *Renewable Energy*, v 16, n 1-4 -4 pt 2, p 749-752, January/April 1999
4. Garg, H.P, Mahajan, R.B.; Sharma, V.K.; Acharya, H.S.: Design and Development of a Simple Solar Dehydrator for Crop Drying, *Energy Conversion and Management*, v 24, n 3, p 229-235, 1984
5. Shemski, S; Bellagi F., Ahmed, S.:Drying of agricultural crops by solar, *Desalination*, v 168, n 1-3, p 101-109, August 15, 2004
6. Supranto S., K.; Daud, W.R.W.; Othman, M.Y.; Yatim, B. Design of an experimental solar assisted dryer for palm oil fronds, *Renewable Energy*, v 16, n 1-4 -4 pt 2, p 643-646, January/April 1999
7. Kreider F. J.; Kreith F.: Solar heating and cooling, Hemisphere Publishing Corporation and McGraw-Hill Book Company (1976)
8. Bergman T., Lavine A., Incropera F., DeWitt D.; Introduction to Heat Transfer, 6th Edition, 2011, Wiley & sons
9. McQuiston F., Parker J., Spitler J.: Heating, Ventilating and Air Conditioning: Analysis and Design, 6th Edition, Wiley & sons 2005